

ADSORPTION ISOTHERM, KINETIC AND THERMODYNAMIC STUDIES FOR REMOVAL OF TOTAL DISSOLVED SOLID FROM PAINT WASTEWATER USING ACID MODIFIED MUCUNA SHELL

^{1*} Okolo B.I., ¹ Oke E. O., ¹ Adeyi O., ¹ Akatobi K.N., ¹ Dzarma G.W.

¹Department of Chemical Engineering Michael Okpara University, Umudike, Nigeria

*Corresponding author. Tel.: +2347032363899; E-mail address: curonokolo@yahoo.com (B.I. Okolo)

ABSTRACT

Present study was conducted to investigate the removal of total dissolved solid (TDS) from paint wastewater (PW) by using eco-friendly biomass of phosphoric acid modified mucuna shell (MSA). Characterization of MSA is done by (i) proximate analysis (ii) surface chemistry by FTIR (iii) surface physical morphology by SEM technique (iv) structural analysis using X-ray diffractometer. Batch experiment was carried out to determine effect of parameters such as pH, biosorbent dose, contact time and temperature. Adsorption capacity of the experimental results was fitted into four isotherm model; Langmuir, Freundlich, Temkin and Dubinin-Radushkevich, but the Freundlich isotherm model was found to have higher correlation coefficient, implying MSA had heterogeneous surface. The adsorption kinetic has been described by pseudo-first-order, pseudo-second-order, Elovich and intra-particle diffusion model. It was observed that the rate of TDS adsorption follow pseudo-second-order model. Free energy of adsorption (ΔG°), enthalpy (ΔH°) and entropy (ΔS°) changes are calculated to know the nature of adsorption. The calculated value of ΔG° at 303K-323K indicates that the adsorption process is spontaneous. From the calculation, values of ΔH° and ΔS° shows positive sign, which indicates that the adsorption process is endothermic in nature and the positive, ΔS° suggested increased randomness at the solid/interface.

Keyword: Paint wastewater, Mucuna shell, Adsorption Isotherm, Adsorption kinetic, Thermodynamics

INTRODUCTION

The increase in industrialization and urbanization has resulted in the production of huge amount of wastewater containing all types of pollutants (El-Sayed, 2011). Latex paints generally consist of organic and inorganic pigments and dyestuffs, extenders cellulosic and non-cellulosic thickeners, latexes, emulsifying agents, anti-foaming agents, preservatives, solvents and coalescing agents (Hedazi; Ajjabi and Chouba, 2009; Aboulhassan et al, 2006; Arami et al, 2005). Therefore, the need for treatment of pant wastewater (PW) for regulatory compliance before discharging becomes imperative. Various techniques have been proposed to treat wastewater containing toxic material/metals (Nguyen et al, 2013; Gomes and Callao, 2005; Gode and Petilivan, 2005). These methods include; chemical oxidation, biological treatment, coagulation-flocculation, Fenton process, sedimentation, adsorption, electrochemical

and membrane processes (Xiong et al, 2009; Liang et al, 2009; Zhang et al, 2013; Khataee and Dehghan, 2011). Among the different treatments available, adsorption is one of the most attractive technologies because of its versatility, simple dosage; ease of operation and high efficiency for pollution removal (Rosales et al, 2012). However, the main drawback of adsorption is the high cost of efficient adsorbent materials. Thus, alterative low-cost adsorbent which requires a porous structure, mechanical and chemical stability, but the manufacturing process and intended applications of the products are also important considerations (Del Rio et al, 2011; Cobas et al, 2014; El-haded, 2012). This has led a growing research interest in the production of activated carbons from renewable and cheaper precursors (Padilla et al, 2013). Large variety of material have been investigated including natural zeolites, sludge, red mud, siliceous material, peat and chitin and chitosan (Liang et al, 2009), poly aluminum hydroxide, clay mineral,

dolomites sorbents (Dogan et al, 2007), magnetic composite, nano particles (Abdulhalim et al, 2011) and organo bentonite (Amosa et al, 2014a). Another alternative was to investigate the possibility of using agro-based inexpensive material as adsorbent. Various kinds of activated carbon have been prepared from low-cost precursor materials, which are predominately vegetable wastes, such as orange peels, melon seed (Adebowale et al, 2008; Ma et al, 2014), coir pith (Banker et al, 2009; Abdolali et al, 2014a), coconut coir (Auta and Hameed, 2011; Krishani et al, 2006), bamboo dust, coconut shell, groundnut shell, rice husk, corncob, almond shell (Nguyen et al, 2013; Gupta and Rastogi, 2009), and palm shell (Ismail et al, 2013; Alothman and Naushad, 2013). (Bansal et al 2009; Park et al, 2005) used rice husk to remove nickel ions from aqueous solution.

Consequently, the scope of this study is not only to prepare chemically cost-effective activated carbon from mucuna shell with H_3PO_4 as an alternative adsorbent for removal of total dissolved solid (TDS) from PW, but also to characterize it and investigate the effects of operating parameters such as solution pH, contact time, amount of adsorbent and temperature. Adsorption isotherm data were fitted to four different isotherm equations such as Langmuir, Freundlich, Temkin and Dubinin-Radushkevich and constants of isotherm equation were determined. Furthermore, four kinetic models including pseudo-first-order, pseudo-second-order, Elovich and intra particle diffusion models were also used to analyze the adsorption kinetics. Thermodynamic parameters such as standard free energy, enthalpy and entropy were also investigated to understand the spontaneity of the adsorption process. Infrared spectra (FTIR), Scanning Electron Microscopy (SEM), X-ray diffraction (XRD) and X-ray fluorescence (XRF) were verified for characterization of mucuna shell adsorbent.

2. Materials and methods

2.1 Material collection

2.1.1 Paint wastewater

The wastewater used in this study was taken from a major paint industry located in Enugu Nigeria, and physicochemical analysis was carried using APHA method of analysis (APHA/AWWA, 1995).

2.1.2 Preparation of biosorbent

Mucuna shell residues, collected from local market in Enugu city, Nigeria, were dried in sunlight and the cut into small pieces. The dried mucuna shell were crushed, washed with 0.5% HCL to remove all dirt, dried in an oven at 105°C, ground, and sieve to mesh size of 1-4mm. It is then carbonized in a furnace at 250°C for 2hr to yield the carbonized mucuna shell residue (MSC).

2.1.2.1 Preparation of H_3PO_4 activated carbon (MSC)

The MSC was soaked in ortho-phosphoric acid solution with the ratio of (1:1 of MSC: H_3PO_4).

The impregnation ratio (IR) was calculated using

$$IR = \frac{W_{H_3PO_4}}{W_{MSC}}$$

1

where, H_3PO_4 is dry weight (g) of ortho Phosphoric acid pellet, and W_{MSC} is dry weight (g) of char.

Then, the impregnated sample is dehydrated in an oven at 110°C, and activated in muffled furnace of 200°C for 1hrs. The obtained H_3PO_4 activated carbon (MSA) was soaked in de-ionized water several times for half an hour with constant stirring after cooling until pH of filtrate reached (6-8). This was followed by drying in an oven at 105°C, and stored in air-tight container for further characterization and adsorption studies. The yield is defined as the dry weight of activated carbon per weight of char utilized for activation.

$$Yield (\%) = \frac{w_c}{w_o} \times 100$$

2

where w_c and w_o are the dry weight of MSA (g) and dry weight of precursor (g), respectively.

2.3 Characterization of materials

2.3.1 Paint wastewater

Standard methods (APHA/AWWA, 1995) were applied to determine the physicochemical and

biological characteristic of the paint wastewater and presented in Table 1.

Table 1: Characteristic result of PW

Parameter	Temp.(^o C)	pH	COD (mg/L)	BOD ₅ (mg/L)	TDS (mg/L)	PO ₄ ⁻ (mg/L)	Colour	E.C (ms/cm)	Turb. (NTU)	TSS (mg/L)	Cl ⁻	SO ₄ ²⁻ (mg/L)
Values	27	7.4	14340	1345	1198.8	6.8	0.034	303.2	100	9532	248	1329.0

2.3.2 MSA sample

Physical and chemical characteristic of MSA, including proximate analysis was determined by ASTM and presented in Table 2 (ASTM D-3172-89). Surface function groups were detected using FTIR

spectrometer (FTIR-84005, SHIMADZU). The surface morphologies of MSA before and after TDS adsorption were identified by using SEM technique (JEOL JSM-6335F, USA). The XRF and XRD pattern of MSA was collected on X-ray powder diffraction (Bruker, D8 Discovery EVA, Germany).

Table 2: Characteristic results of MSA

Carbon sample	Moisture content %	Ash content %	Surface area (mg/g)	Bulk density (g/cm ³)	Iodine number (mg/g)	Yield %	Point of zero charge
MSA	3.64	4.86	864.02	0.39	864.53	21.43	8.51

3 Batch adsorption experiments

Batch experiments were performed to determine adsorption isotherm, kinetic and thermodynamic parameters of TDS adsorption on MSA, as a function of initial pH, contact time, temperature and adsorbent dosage. The adsorption experiments were carried out by adding MSA into 250-ml Erlenmeyer flask with glass stoppers, containing 50ml of PW solution with a fixed concentration of 181mg/L at 30°C. The flasks were shaken in a thermostatic mechanical shaker (HAAKE SWB20, Fission Ltd Germany) for 30mins. At the end of each run and before measurement of residual TDS, all samples were centrifuged for 10mins using a centrifuge (Sigma-301, Germany) with a speed of 3500rpm and then passed through a filter paper Whatman 42. The absorbance of the supernatant was estimated to determine the residual TDS concentration, and was measured before

and after treatment using UV-vis spectrophotometer (UV-1650A, Shimadzu, Japan) at λ_{max} 560nm. To increase the accuracy, all experiments were done in triplicate basis. The effect of pH was observed by studying the adsorption of TDS over the pH range from 2-10. The pH of PW solution was adjusted by using NaOH or HCL solution and was determined using pH meter (HACH 103). The adsorption studies were carried out at different temperature (30°, 40°, 50°C). This is used to determine the effect of temperature on the thermodynamic parameters. The amount of adsorption at time t, q_t (mg/g), was calculated using the following formula.

$$q_t = \frac{(C_o - C_t)V}{m} \quad 3$$

where C_t (mg/L) is the liquid phase concentrations of PW at any time, C_o (mg/L) is the initial concentration

of the TDS in PW solution, V is the volume of the solution (L) and m is the mass of dry adsorbent (g).

The amount of equilibrium adsorption, q_e (mg/g) was calculated using the formula

$$q_e = \frac{(C_o - C_e)V}{m} \quad 4$$

Where, C_o and C_e (mg/g) are the liquid phase concentrations of TDS initially and at equilibrium.

The TDS removal percentage can be calculated as follows,

$$\% \text{ of TDS removal} = \frac{C_o - C_e}{C_o} \times 100 \quad 5$$

where C_o and C_e (mg/L) are the initial and equilibrium concentration of the TDS in PW solution (Shama and Gad, 2013).

3 Results and discussion

3.1 Characterization results

3.1.1 Physiochemical and biological characteristics of PW and MSA

The physiochemical and biological characteristics of PW used in this study were presented in Table 1. From the results, it can be seen that total suspended solid (TSS), total dissolved solid (TDS), carbon oxygen demand (COD) and biological oxygen demand (BOD) contributing to the perceived turbidity of PW. With this, it is significant enough for the application of adsorption process towards the removal of TDS from PW. From Table 2, the higher surface area (864.02mg/g) and low ash content associated with MSA was an indication of a greater adsorptive potential (Hossain et al, 2012). Since iodine number is the most fundamental parameter used to characterize activated carbon performance, it is a measure of activity level; higher number of iodine, indicates higher degree of activation (Table 2). This agrees with previous work (Ademiuyi et al, 2009). To understand the adsorption mechanism it is necessary to determine the point of zero charge (pH_{zpc}) of the adsorption. The point of intersection of the resulting curve with abscissa, where pH was zero, gives the pH_{zpc} . Adsorption of cations is favoured at $pH > pH_{zpc}$ while the adsorption of anions is favoured at $pH < pH_{zpc}$ (Budinova et al, 2006). In this work, pH_{zpc} for MSA is 8.51 This result is shown in Fig 1.

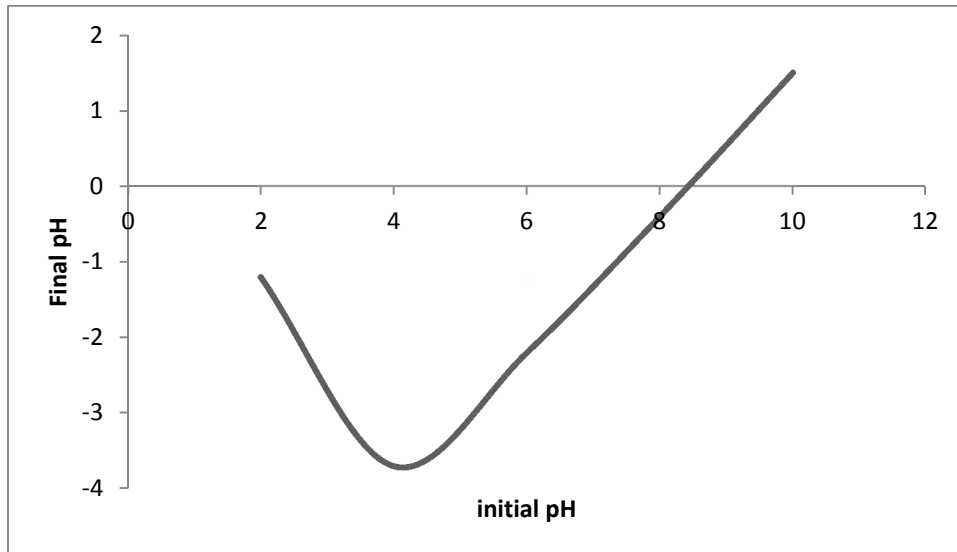


Fig. 1. Point of zero charge (pH_{zpc}) of MSA used for the adsorption of TDS

3.1.2 FTIR spectral analysis

The FTIR analysis was used to identify the different functional groups present in MSA. Fig. 2a and b, shows the functional groups according to their corresponding wave number before and after adsorption (Fomkin, 2009). Chemical modification in general improved the adsorption capacity of adsorbent. The MSA surface is oxidized by treatment with phosphoric acid (H_3PO_4) leading to the generation of HPO_4 type carbon functional groups which bear significance in the redox chemistry of carbon materials (Attia et al, 2006). From Fig 2a and b, the adsorption peaks at 3429.43cm^{-1} indicates the existence of free hydroxyl groups in water. The band located at 879.54cm^{-1} associated with HPO_4^{-2} ions due to the stretching vibration of the link PO (H). The band located at 879.54 associated with HPO_4^{-2} ions, is found to be shifted to 877.61cm^{-1} after adsorption, this may be responsible for the chemical interaction of the TDS with HPO_4^{-2} group in MSA. The peaks 1346.31 to 1043.49cm^{-1} was due to $-C-O$ stretching in alcohols, phenols, ether, ester, acids lactose's and carboxyl anhydrides (NageswaraRao et al, 2011). The peaks at $1874-1757\text{cm}^{-1}$ pertaining to the $-C=O$ stretching in

carbonyl and carboxyl groups and in lactones (Dai Fullah et al, 2007). The peak 1757.15cm^{-1} corresponds to the $C=O$ stretching that may be attributed to the hemicelluloses and lignin aromatic group (Jambulingam et al, 2007). The $C=C$ stretching vibration between $1566.13-1654.92\text{cm}^{-1}$ is indicative of alkenes and aromatic functional groups (Mall et al, 2006). Peaks detected at $1000-1100\text{cm}^{-1}$ in the spectrum of the activated carbon prepared, represents the presence of $C-O-C$ stretching vibrations of esters, ether or phenol groups whereas the weak to medium peaks located at $428.20-879.54\text{cm}^{-1}$ is assigned for $C-H$ out-of plane bending of benzene derivatives, OH stretching vibrations of $C-O-H$ band. The results obtained agreed with the previous results where $C-H$ out-of plane bending vibration for benzene derivatives were found on the surface of various activated carbon (Prahas et al, 2008). Therefore, from the above results, it can be concluded that HPO_4^{-2} and PO_4^{3-} group are involved in the interaction with TDS. The analysis of FTIR shows that the functional group contributes to the adsorption of TDS on the surface of MSA (Prahas et al, 2008; Yun et al, 2008; Garg et al, 2009).

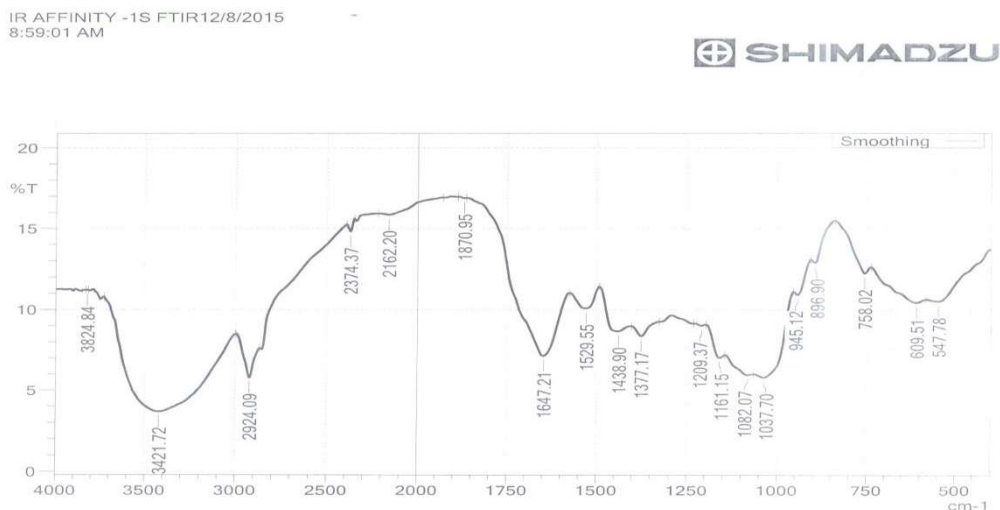


Fig 2a: FTIR spectrum analysis of MSA adsorbent before adsorption of TDS in PW

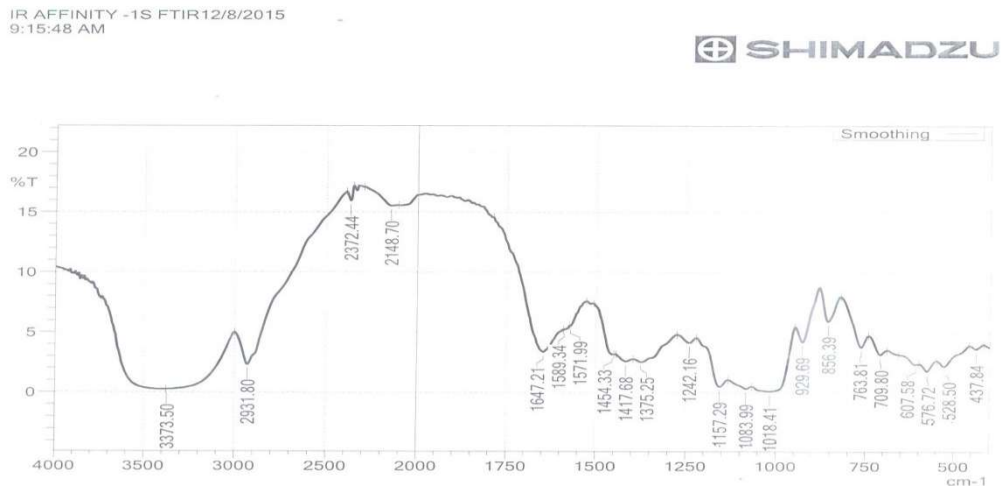
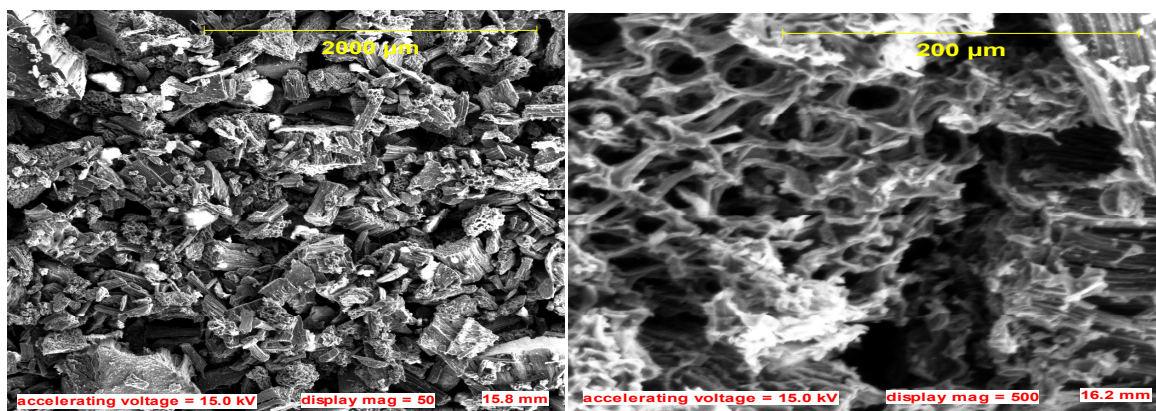


Fig 2b: FTIR spectrum analysis of MSA adsorbent after adsorption of TDS in PW

3.1.3 Scanning electron microscopy (SEM)

The prepared activated carbon was examined by using scanning electron microscopy JEOL (JSM-6480LV) to analyze the surface of the adsorbent. A significant pore structure exists with a series of rough cavities distributed over the surface of MSA. This was due to the breakdown of Lignocellulose at high temperature of volatile compounds leaving samples with well - developed pores .Fig 3 presents the SEM micrograph illustrating the morphology of the adsorbent (MSA) before (A) and after (B) adsorption of TDS in PW.

After modification with H_3PO_4 , many various sizes of pores in a honey comb can be observed on the surface of MSA after adsorption. The micrograph after adsorption of TDS, had their surface covered with irregular adhered substances which were suspected to be the adsorbate molecules (TDS), unlike the structure of the adsorbent (MSA) before adsorption which had a clear plain surface. Similar types of pore arrangement were observed in the activated carbon prepared from palm fiber jute and coconut fibers (Tan et al, 2008; Phan et al, 2006).



Before

After

Fig 3: SEM micrographs of mucuma shell acid (MAS) treated adsorbent before and after adsorption

3.1.4 X-ray Diffraction Analysis

X-ray diffraction technique is a powerful tool used to analyze the crystalline nature of materials. If the material under investigation is crystalline, well defined peaks are observed, while non-crystalline or amorphous system shows hallow instead of a well-defined peaks.

In this study, the identification of the mineralogical constituents and phase properties of MSA was conducted by X-ray diffractometer (XRD-6000 SHIMADZU, Japan) and illustrated in Fig. 4 This is done at 2θ value between 10° and 80° at scan rate of 2 degree per minute. Thus MSA has a completely

amorphous structure which is expected for organic materials. The broad peaks and absence of sharp peaks, reveals predominantly amorphous structure which is an advantageous property of well-defined porous adsorbent (Valenta Nabais et al, 2009). The X-ray diffraction pattern of MSA, shows the presence of intense lines characteristics of Mica/Illites, kaolinite and quartz. The reflection associated with Mica/Illites is characterized by reflection located at $2\theta = 17^\circ$ and 25° and kaolinite at $2\theta = 20^\circ$ and 21° , while Mica/Illites was located at 17° , 18° and 24° and kaolinite at 20° and 22° . This result was also reported by other researchers (Valenta Nabais et al, 2009).

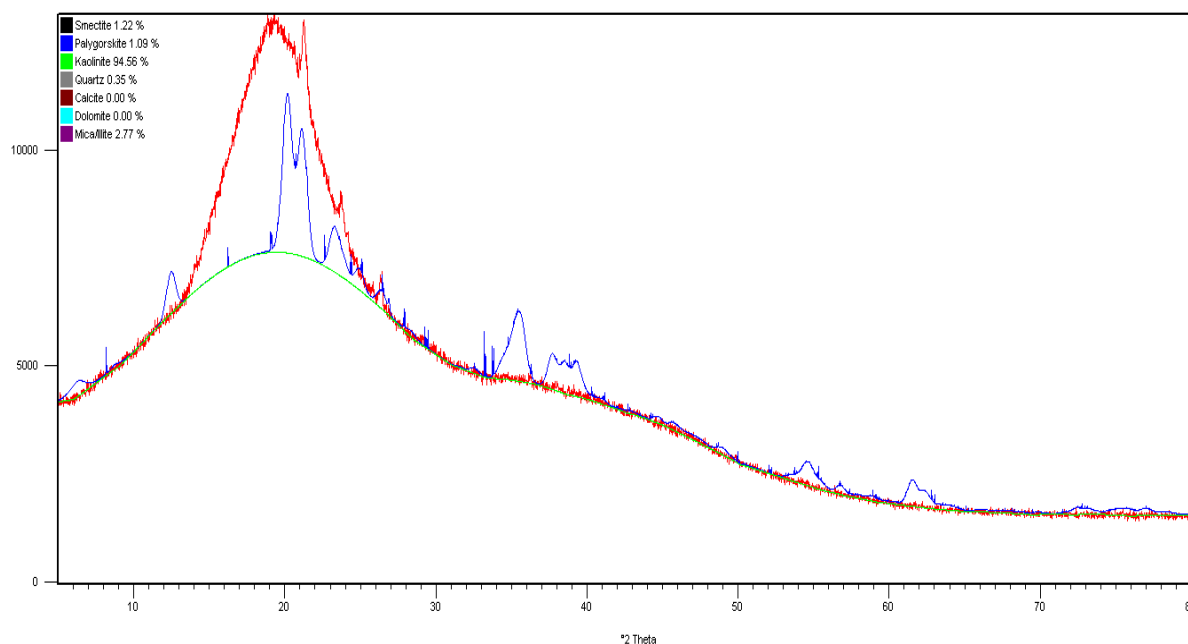


Fig 4: X-ray diffraction pattern of mucuna shell acid (MSA) treated adsorbent

3.2.1 Effect of dosage

To investigate the effect of dosage, experiments were conducted by varying adsorbent mass (20-100mg) at fixed initial concentration of 181mg/L. The biosorption of TDS as shown in Fig.5 increases with an increase in biosorbent dosage. Such behavior is obvious because with an increase in biosorbent dosage, the number of active sites available for TDS

would be more. As time increases, more amounts of TDS gets adsorbed onto the surface of the biosorbent due to Vander Waals forces of attraction and result in decrease of available surface area. The adsorbates normally form a thin one molecule thick layer over the surface. When this monomolecular layer covers, the capacity of the biosorbent is exhausted (Nnadi et al, 2009; Bhattacharya et al, 2005; Ozacar et al, 2003).

3.2.2 Effect of pH

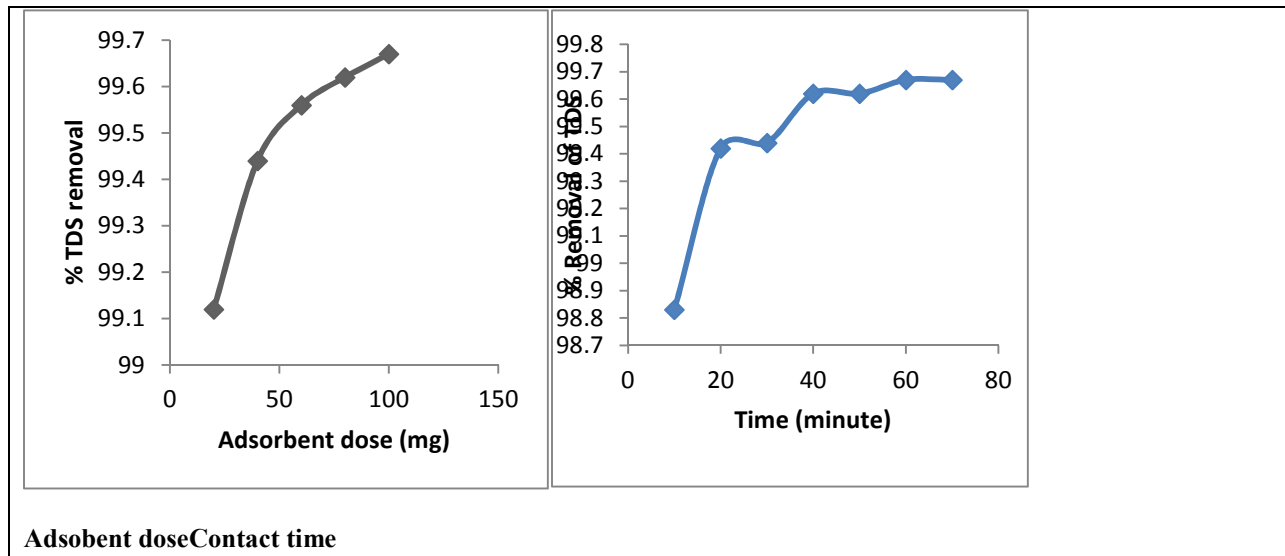
Solution pH is an important monitoring parameter influencing the adsorption behavior of adsorbate onto biosorbent surface due to its impact on both the surface binding sites of the biosorbent and the metal ion solution. In the present study, the effect of pH on biosorption of TDS onto MSA was studied in a range of 2-10 and was shown in Fig. 5. The 99.75% removal of TDS was observed at pH 8, indicating that the biosorption was strongly pH dependent. The pH_{zpc} value of MSA was determined as 8.51 (Fig.1). At $pH < pH_{zpc}$, the carbon surface has a net negative charge (Ajjabi and Chouba, 2009; Ozacar et al, 2003; Senthilkumar et al, 2006). At pH 2, a significantly high electrostatic attraction exists between negatively charged TDS ions and MSA surface. At low pH, the cations compete with the H^+ ions in the solution for active sites and therefore lower adsorption (Lugo-Lugo et al, 2009).

3.2.3 Effect of contact time

The uptake of TDS as a function of contact time is shown in Fig.5. The removal rate was rapid initially and then gradually diminished to attain an equilibrium time beyond which there was no significant increase in the rate of removal. Hence, in this work, 40min was chosen as the equilibrium time. The fast adsorption rate at the initial stage may be explained by an increased availability in the number of active binding sites on the adsorbent surface.

3.2.3 Effect of temperature

The temperature dependence of the adsorption process is related with several thermodynamic parameters. The temperature effect on removal of TDS from PW using MSA was studied by conducting the experiment at different temperature 303, 313, 323K. Fig 5 shows that the adsorption capacity increases from 97.4 to 99.37% with an increase in temperature. This suggests that the adsorption process is endothermic in nature. This may be due to the increase in the TDS mobility to penetrate inside the MSA pores at high temperature (Hashem et al, 2007; Larous et al, 2005).



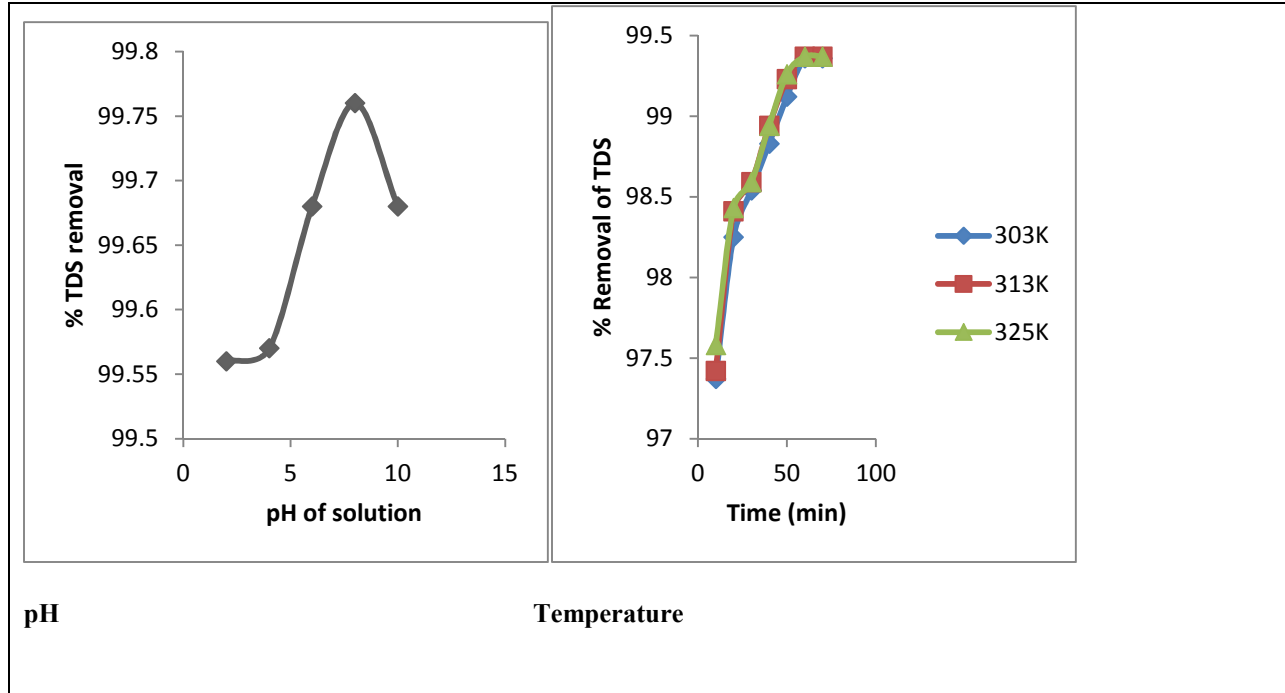


Fig. 5 Effect of various parameters. Adsorbent dosage, pH, contact time, temperature on the adsorption of TDS onto MSA (left to right).

3.3 Adsorption isotherms

The adsorption isotherm gives a picture of the distribution of adsorbate species between aqueous and solid phase-over the adsorbent surface at equilibrium state (Singanan , 2011). Several equilibrium models have been developed to describe adsorption isotherm relationships. The data obtained were analyzed with Langmuir, Freundlich, Tempkin and Dubinin-Radushkevich isotherm equations (Langmuir, 1961, Khan et al, 2009; Babel and Kurniawan, 2003; Namasivaayam and Kavith, 2002). The sorption isotherm is the mathematical model, which gives an explication for the adsorbate species behaviour between liquid and solid phases [Ghoniem et al, 2014][].

3.3.1 Langmuir isotherm model

The Langmuir isotherm model [88], was used to describe observed adsorption phenomena and suggest that uptake occurs on a homogeneous surface by monolayer adsorption without interaction between adsorbed molecules. Based upon this assumption, Langmuir represented the following equation:

$$q_e = \frac{q_{max}K_L C_e}{1+K_L C_e}$$

6

Langmuir adsorption parameters were obtained by transforming equation (6) into linear form

$$\frac{1}{q_{eq}} = \frac{1}{q_{max}K_L C_e} + \frac{1}{q_{max}}$$

7

where C_e is the equilibrium concentration of TDS (mg/L), q_{eq} is the amount of TDS adsorbed per specific amount of adsorbent (mg/L), q_{max} is the maximum adsorption capacity (mg/L), and K_L is an equilibrium constant (L/mg). q_{max} and K_L can be determined from the linear plot of $1/q_{eq}$ vs $1/C_e$ shown in Fig 6.

The slope of the Langmuir isotherm can be used to predict whether adsorption system is favorable or unfavorable in a batch adsorption process. The essential features of the isotherm can be expressed in terms of a dimensionless constant separation factor

(R_L) that can be defined by the following relationship (Hema and Arivoli, 2007).

$$R_L = \frac{1}{1 + K_L C_i}$$

8

The value of separation parameter R_L provides important information about the nature of adsorption. The value of R_L indicated the type of Langmuir isotherm to be irreversible ($R_L = 0$), favourable ($0 < R_L < 1$), linear ($R_L = 1$) or unfavourable ($R_L > 1$). It can be explained that when $K_L > 0$, adsorption system is favourable (Ozcimen and Ersoy-Meridooyu, 2010). From the data calculated in table 4, the R_L is greater than 0 but less than 1 indicating that Langmuir isotherm is favourable. From this study, the maximum monolayer coverage capacity q_{max} from Langmuir isotherm model was determined to be 83.33mg/g, K_L is 0.189L/mg, R_L (separation factor) is 0.081 indicating that the equilibrium sorption was favourable and R^2 value is 0.8648 proving that the sorption data fitted well to Langmuir isotherm model.

3.3.2 Freundlich isotherm model

Freundlich isotherm (Freundlich, 1906) is based on multilayer adsorption onto heterogeneous surface with a uniform energy distribution and reversible adsorption [92].

The Freundlich isotherm is represented by:

$$q_e = K_f C_e^{1/n} \tag{9}$$

Here K_f is an approximate indicator of adsorption capacity, while $1/n$ is a function of the strength of adsorption in the adsorption process, q_e is the amount of TDS adsorbed at equilibrium and C_e is the residual concentration of TDS in solution. Linearizing equation 9, we have

$$\log q_e = \log K_f + \frac{1}{n} \log C_e \tag{10}$$

The constant K_f is an approximate indicator of adsorption capacity, while $1/n$ is a function of the strength of adsorption in the adsorption process (Krishnan et al, 2010). The values of K_f and n can be obtained from intercept and slope of a plot of $\log q_e$ versus $\log C_e$ (Fig. 6). The adsorption data calculated are presented in Table 4. If value of $1/n$ is below 1, it indicates a normal adsorption (Krishnan et al, 2010). From the data in the Table 4, the value of $1/n = 0.3719$ while $n = 2.688$ indicating that the adsorption is favourable and the R^2 value is 0.9146. The data is best represented by Freundlich isotherm.

3.3.3 Tempkin isotherm model

This isotherm contains a factor that explicitly taking into account of adsorbent-adsorbate interactions. By ignoring the extremely low and large value of concentrations, the model assures that heat of adsorption of all molecules in the layer would decrease linearly rather than logarithmic with coverage (Temkim and Pyzhev, 1940; Yaswmin and Zeki, 2007). As implied in the equation, its derivation is characterized by a uniform distribution of binding energies which was carried out by plotting the quantity adsorbed q_e against $\ln C_e$ and the constants were determined from the slope and intercept (Fig.6) Tempkin isotherm model is given by the following equations :

$$q_e = \frac{RT}{b} \ln(A_T C_e)$$

$$q_e = \frac{RT}{b_T} \ln A_T + \left(\frac{RT}{b}\right) \ln C_e$$

$$B = \frac{RT}{b_T}$$

$$q_e = B \ln A_T + B \ln C_e \tag{11}$$

Where A_T is Tempkin isotherm equilibrium binding constant (L/g), b_T Tempkin isotherm constant, R universal gas constant (8.314J/mol/K), T temperature (K), B constant related to heat of adsorption (J/mol).

From the plot shown in Fig. 6 and Table 4, the following values were obtained. $A_T = 2.556$ L/g, $b_T =$

179.66 J/mol, which is an indication of heat of adsorption indicating physical adsorption process and the $R^2 = 0.8358$

3.3.4 Dubinin- Radushkevich isotherm model

D-R model (Dubinin and Radushkevich, 1947) was chosen to estimate the heterogeneity of the surface energies and also to determine the nature of biosorption process as physical or chemical. The D-R adsorption isotherm does not assume a homogeneous surface or constant adsorption potential. It is commonly applied in the following form

$$\ln q_e = \ln q_m - K_{ad}\epsilon^2$$

12

Where q_e is amount of adsorbate on the adsorbent at equilibrium (mg/g), q_m is theoretical isotherm saturation capacity (mg/g), K_{ad} is Dubinin-Radushkevich isotherm constant (mol^2/KJ^2) and ϵ^2 is the Polanyi potential given by the relation (Dubinin and Radushkevich, 1947; Jaman et al, 2009) :

$$\epsilon = RT \ln \left[1 + \frac{1}{C_e} \right]$$

13

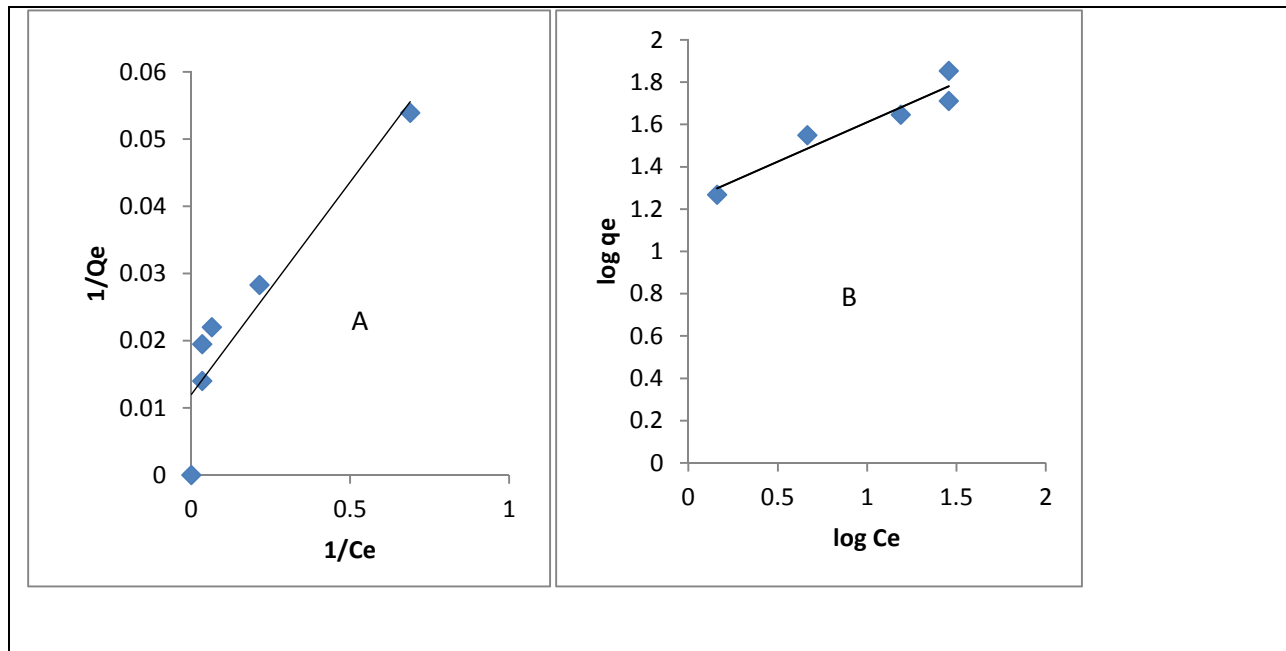
Where C_e is the equilibrium concentration of adsorbate in solution (molL^{-1}), R is universal gas constant ($\text{Jmol}^{-1}\text{K}^{-1}$) and T is the absolute temperature (K). The D-R constants q_m and K_{ad} were calculated from linear plots of $\ln q_e$ versus ϵ^2 as shown in Fig.6 and are given in Table 4. The constant K_{ad} gives an idea about the mean free energy E (KJ mol^{-1}) (Hussans and Khan et al, 2011).

The adsorption energy can also be worked out using the following relationship:

$$E = \frac{1}{\sqrt{2K_{ad}}}$$

14

Where, E is the mean free energy of adsorption. If the value of E is between 1 and 16KJmole, then physical adsorption prevails and if it is more than 16 KJmol, then chemisorption prevail. The value of E calculated is 912.87KJ/mol, which indicates that chemisorption process plays the significant role in the adsorption of TDS onto MSA.



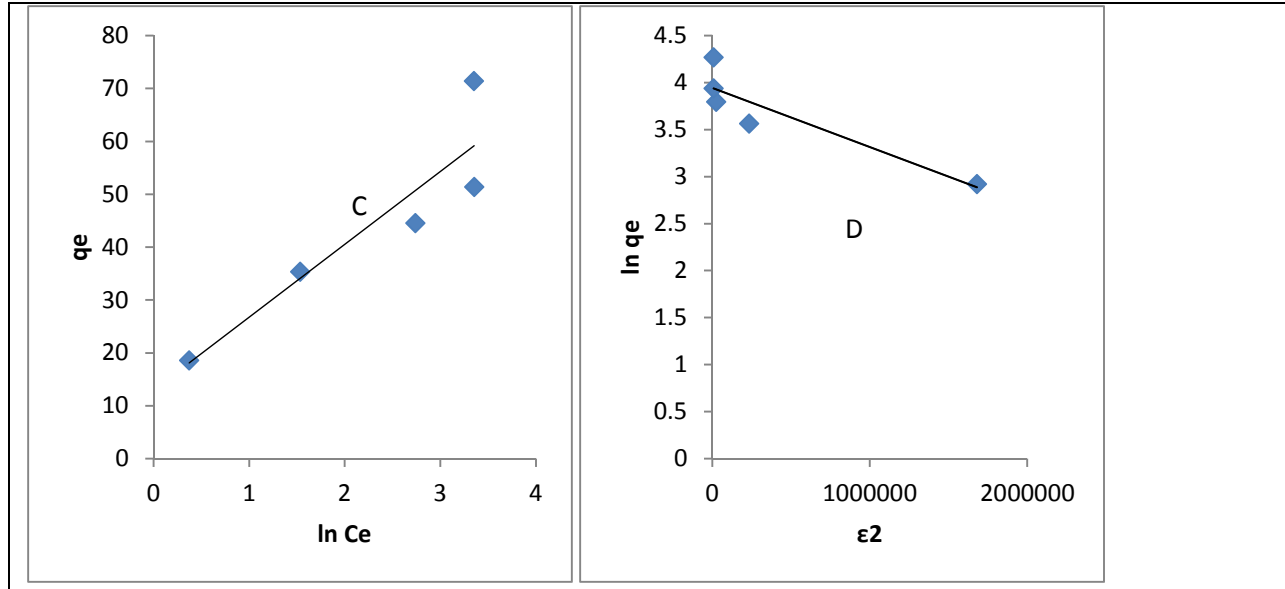


Fig.6 A, B, C, D shows Langmuir, Freundlich, Dubinin-Radushkevich and Temkin adsorption isotherm respectively.

Table 4 Langmuir, Freundlich, Temkin and Dubinin-Radushkevich Isotherm constant for the adsorption of TDS onto MSA

Langmuir				Freundlich			
$q_{max} \text{ mg/g}$	$K_L \text{ (L/mg)}$	R_L	R^2	1/n	n	$K_f \text{ mg/g}$	R^2
83.33	0.189	0.081	0.8643	0.3719	2.69	17.34	0.9146
Temkin				Dubinin-Radushkevich			
$A_T \text{ (L/mg)}$	b_T	B (mg/g)	R^2	$q_s \text{ (mg/g)}$	$K_{ad} \text{ (mol}^2\text{)}$	E	R^2
2.556	179.66	13.79	0.8358	51.563	6×10^{-7}	912.87	0.8225

3.4 Adsorption Kinetics

The kinetic of adsorption describes the solute uptake rate, and this rate controls the habitation time of adsorbate uptake at the solid-solution interface. The kinetic gives information about reaction pathways and time to reach equilibrium. It is one of the important characteristics in defining the efficiency of adsorption (Aman et al, 2008). In this study, some kinetic models namely pseudo-first order, pseudo-second order,

Elovich and intra-particle diffusion model are investigated to find the best fitted model for the experimental data.

3.4.1 Pseudo-first order model

The pseudo-first order rate expression, popularly known as the Lagergren equation, is generally described by the following equation (Srivasta et al, 2006; Remero-Gonzalez, 2005; Oguz, 2005).

$$\frac{dq}{dt} = K_1(q_e - q_t) \quad 14$$

Where q_e the amount of TDS as is adsorbed at equilibrium per unit weight of adsorbent (mg/g), q_t is the amount of TDS adsorbed at any time (mg/g), and K_1 is the rate constant (min^{-1}). Integrating and applying the boundary conditions from $t=0$ and $q=0$ to $t=t$ and $q = q_t$

Equation (14) takes the form

$$\ln(q_e - q_t) = \ln q_e - K_1 t \quad 14$$

The plot of $\ln(q_e - q_t)$ versus t (as shown in Fig.7) should give a straight line with slope of K_1 and intercept $\ln q_e$, were used to determine pseudo first order rate constant (K_1) and theoretical amount of TDS adsorbed per unit mass of adsorbent $q_e(th)$, were compared with the $q_e (exp)$ values in Table 5. The $q_e (exp.)$ values differ from the corresponding $q_e (th)$ values showed that pseudo-first order model does not fit well with whole range of contact time, and hence not diffusion- controlled phenomena.

3.4.2 Pseudo-second order model

The pseudo-second order kinetic model states that the interaction between solute and adsorbate molecules may be chemical forces of attraction on the solid surface of the adsorbent and adsorbate molecules (Ismail et al, 2013). The mathematical form of the expression:

$$\frac{dq_t}{dt} = K_2(q_e - q_t)^2 \quad 15$$

Where, K_2 is pseudo-second order rate constant (g/mg.min). After integrating, equation (15) for boundary conditions $q_t = 0$ at $t=0$ and $q_t = q_t$ at $t=t$, the following equation is obtained.

$$\frac{t}{q_t} = \frac{1}{K_2 q_e^2} + \frac{1}{q_e} t \quad 16$$

Fig.7 shows that the plot of t/q_t versus t is a straight line with slope $1/q_e$ and intercept $1/K_2 q_e^2$. Using the value of q_e calculated from the slope, the value of K_2 is determined from the intercept. The calculated value of K_2, q_e and their corresponding regression coefficient (R^2) values are presented in Table 5. On

the other hand, the pseudo-second-order model shown in Table 5, fits the kinetic better, as their correlation coefficient is close to 1 (0.999). The estimated value of q_{cal} are also close to the experimental q_{exp} . Thus, it may be concluded that the adsorption of TDS on MSA can be better explained by pseudo-second-order kinetic model than that of first-order kinetic model and the process is chemisorption controlled.

3.4.3 Elovich Kinetic Equation

The Elovich model equation is generally expressed as:

$$\frac{dq_t}{dt} = \alpha \exp^{-\beta q_t} \quad 17$$

Where α is the initial adsorption rate (mg/g min) and β is the adsorption constant (g/mg) during any experiment. To simplify the Elovich equation by applying the boundary conditions $q_t = 0$ at $t = 0$ and $q_t = q_t$ at $t = t$, equation 17 becomes:

$$q_t = \frac{1}{\beta} \ln(\alpha\beta) + \frac{1}{\beta} \ln(t) \quad 18$$

If TDS adsorption fits the Elovich model, a plot of q_t versus $\ln(t)$ should yield a linear relationship with a slope of $(\frac{1}{\beta})$ and an intercept $(\frac{1}{\beta}) \ln(\alpha\beta)$. The slope and intercept were used to determine the constant β and the initial adsorption rate α . The plot is shown in Fig.7 and the constants obtained presented in Table 5.

3.4.4 Intraparticle Diffusion Model

The adsorption of TDS on MSA is the combination of four consecutive steps, diffusion in the bulk solution, and then diffusion across the thin film surrounding the adsorbent particles, followed by intra-particle diffusion and adsorption within the particles. Weber and Morris intra-particle model was used to elucidate the diffusion mechanism. The model is expressed as:

$$q_t = K_{ad} t^{1/2} + C \quad 19$$

Where, q_t is the amount of TDS adsorbed, t is the contact time, C is the intercept and K_{ad} is the intra-particle diffusion rate constant. A plot of q_t versus $t^{1/2}$ shown in Fig. 7, gives a straight line with positive intercept for intra-particle diffusion

controlled adsorption process, but does not pass through origin due to boundary layer effect. The high value of K_{ad} and intercept, illustrate an enhancement in the rate of adsorption. When the intercept is large,

the greater the contribution of surface adsorption in rate determining step. The results of the constants are presented in Table 5

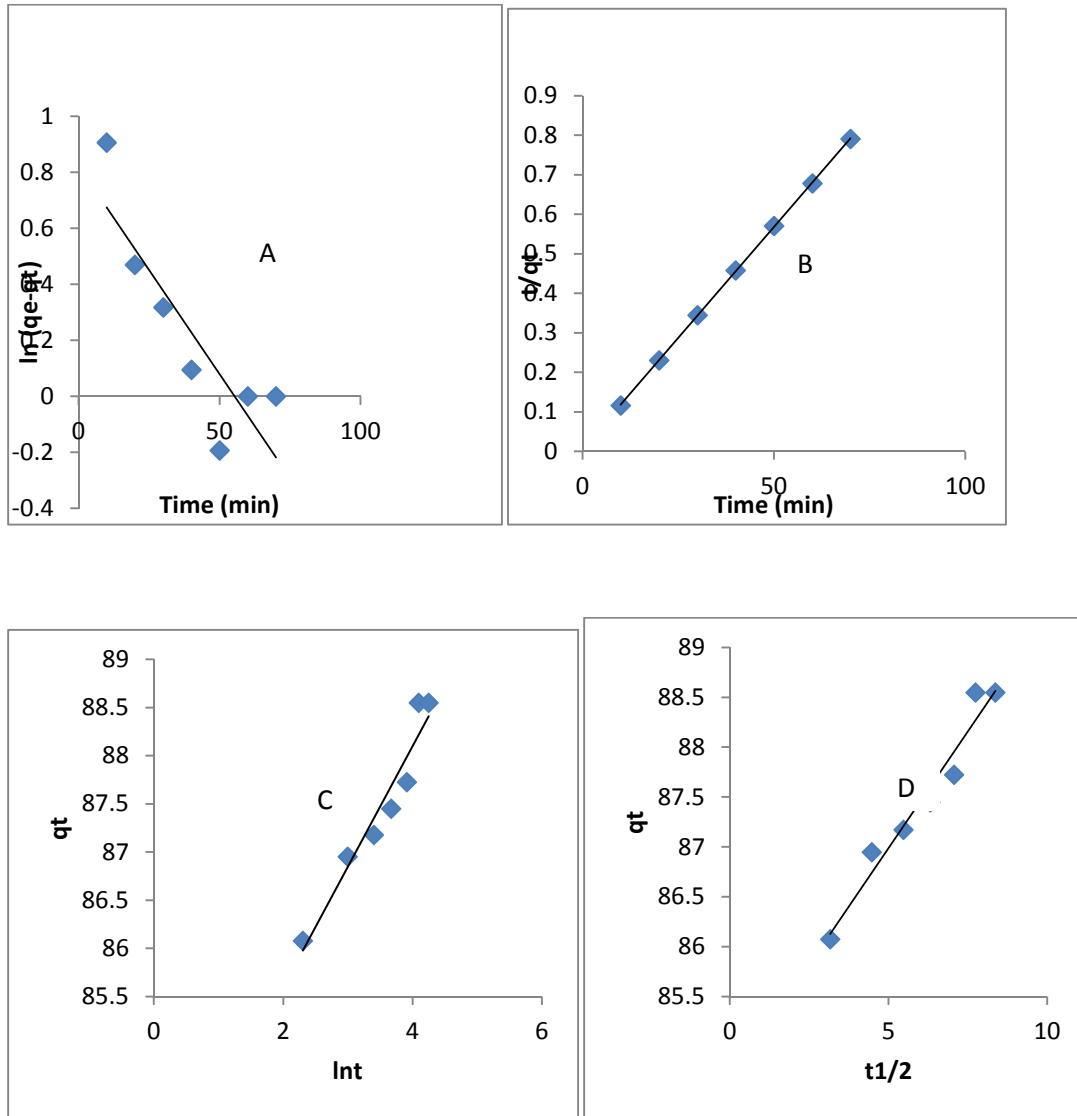


Fig. 7 A, B, C, D Pseudo-first-order, pseudo-second-order, Elovich and intra-particle diffusion model .

The experimental data revealed that of the four kinetic models, namely, pseudo-first-order, pseudo-second-order, Elovich and Weber and Morris intra-particle diffusion model when correlated with the linear forms, the correlation coefficient value of $R^2 = 0.999$ for the pseudo-second-order is the best fit to the experimental data of the present studied adsorption system. The next

to follow the order is the intra-particle diffusion model with $R^2 = 0.9566$, Elovich model with $R^2 = 0.9345$ and the least is pseudo-first-order with $R^2 = 0.7526$. The correlation coefficient of $R^2 = 0.9345$ value for the Elovich model suggest that the diffusion of the TDS follow the Elovich kinetic pattern and the rate determining step is diffusion in nature. The low

correlation coefficient value of $R^2 = 0.7526$ for pseudo-first-order indicates that the model does not apply to the present studied adsorption system.

Table 5 Kinetic parameter for the adsorption of TDS onto MSA

Pseudo-first order				Pseudo-second-order			
$q_e cal.$ mg/g	$K_1 min^{-1}$	$q_e exp. mg$ /g	R^2	$q_e cal.$ mg/g	K_2 g/mg/min	$q_e exp.$ mg/g	R^2
2.279	0.0149	88.075	0.7526	89.286	0.0209	88.075	0.9999
Elovich model			Intra-particles diffusion				
β g/mg	α mg/g	R^2	A	$K_i min^{-1}$	R^2		
0.8013	1.2668	0.9345	84.65	0.4681	0.9566		

3.5 Thermodynamic study

Thermodynamic study for the adsorption of TDS onto MSA adsorbent was conducted in the temperature range of 30-50°C (Nethayi et al, 2010). Thermodynamic parameters for this uptake process such as change in free energy (ΔG), change in enthalpy (ΔH) and change in entropy (ΔS) was calculated using the following equations (Weng and Huang, 2004; Chen and Zhao, 2009).

$$K_c = C_{AC}/C_e \quad 20$$

Where K_c the equilibrium constant, C_{AC} and C_e are the equilibrium concentration (mg/L) of the TDS

adsorbed and left in the solution, respectively. ΔG was calculated using the following relationship

$$\Delta G = \Delta G^o + RT \ln K_c \quad 21$$

At equilibrium, $\Delta G = 0$, thus

$$\Delta G^o = -RT \ln K_c \quad 22$$

Where T is absolute temperature in kelvin, and R is the gas constant.

ΔH^o was calculated from the following equations

$$\Delta G^o = \Delta H^o - T\Delta S^o \quad 23$$

$$\ln K_c = \Delta S^o/R - \Delta H^o/RT \quad 24$$

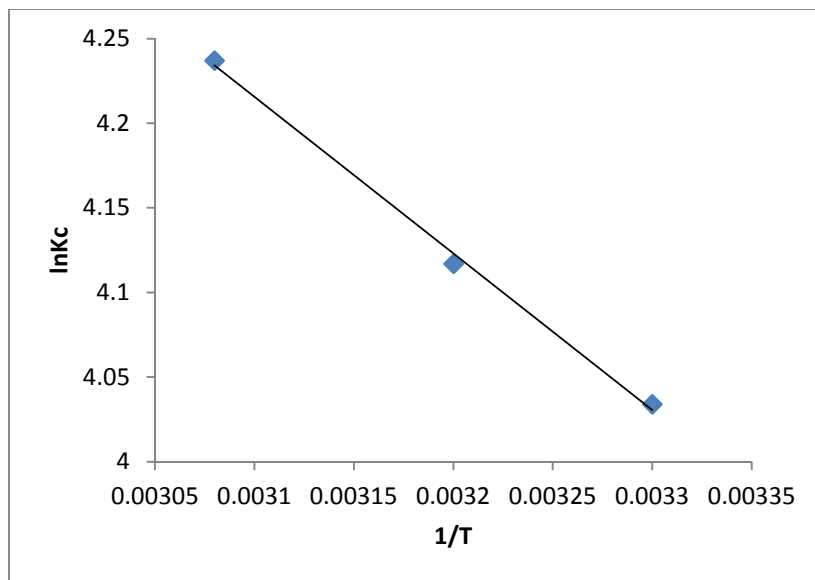


Fig. 8 Van't Hoff plot of TDS adsorption onto MSA

Table 6 Thermodynamic Parameters for the adsorption of TDS on MSA

ΔH° (KJmol)	ΔS° (Jmol)	R^2	ΔG° (KJmol)		
			303K	313K	323K
545.6	3.721	0.9973	-581.96	-619.17	-652.83

The enthalpy change (ΔH°), and the entropy change (ΔS°) were calculated from the slope and the intercept in linear plots of $\ln K_c$ versus $1/T$ as shown in Fig 8. The values of the thermodynamic parameters ΔH° , ΔS° and ΔG° for TDS uptake onto MSA were calculated using equation 23 and given in Table 6. The free energy change (ΔG°) indicates the degree of spontaneity of the adsorption process and the higher negative value reflects a more energetically favorable adsorption. As the temperature increased, the ΔG° value increased indicating a higher driving force resulting in a greater adsorption affinity at higher temperature [106]. The positive value of ΔH° shown in the table, confirmed the endothermic nature of the adsorbent for TDS adsorption in the studied range 303-323K. The positive value of ΔS° suggested increased randomness at the solid/solution interface with some structural changes in the adsorbate and adsorbent, and an affinity of the adsorbent toward

TDS. Other researches have reported similar results (Dio et al, 2002; Haimour and Emeish, 2006; Bhatanager and Sillanpaa, 2010; Safa and Bhatti, 2011a; Ketcha et al, 2012).

4 Conclusions

This research indicated that the mucuna shell activated (MSA) could be used as an effective adsorbent material for the removal of TDS from paint wastewater (PW). Characterization of the activated carbon adsorbent through FTIR, XRD, XRF and SEM techniques confirmed the adsorption of TDS on the adsorbent surface. The adsorption data fitted into Langmuir, Freundlich, Tempkin and Dubinin-Rachkevich isotherms out of which Freundlich adsorption model was found to have the highest correlation coefficient ($R^2=0.9868$). In kinetic studies, pseudo-first first order, pseudo-second order, Weber

and Morris intra particle diffusion model and Elovich equation were applied to identify the rate and kinetic of adsorption process. The adsorption process had good correlation coefficient values with pseudo-second order, showing that the process fitted best with pseudo-second-order model. The estimated thermodynamic parameters established the suitability of TDS adsorption process. The negative ΔG° values confirm the feasibility of the adsorption process and the spontaneous nature of TDS adsorption onto the adsorbent. The more negative values of ΔG° with the rise in temperature imply a greater driving force to the adsorption process and show an increase in feasibility of adsorption at higher temperature. The positive values of enthalpy change ΔH° confirm the endothermic nature of TDS adsorption on MSA adsorbent. The positive value of ΔS° showed the increased randomness of the adsorbate molecules on the solid surfaces than in the solution. Thus, activated carbon prepared from mucuna shell with H_3PO_4 activation can be applied for the treatment of paint wastewater (PW). MSA showed a good potential for TDS removal and its application is economical than commercial activated carbon.

References

- Abdulhalim A., N.N. ZainaAbidin, N. Awang, A. Ithnin, M. Othman and M.Wahab, (2011). Ammonia and COD removal from synthetic leachate using rice husk composite adsorbent. *J. Urban Environ.Eng*,5 24-31
- Abdolali A., W.S. Guo, H.H. Ngo, S.S. Chen, N.C. Nguyen, K.L. Tung, (2014a). Typical Lignocellulosic waste and by-products for biosorption process in water and wastewater treatment: a critical review. *Bioresour. Technol.* 160, 57-66.
- Aboulhassan M. A, S. Souabi, A. Yaacoubi, M. Baudu.,(2006). Improvement of paint effluent coagulation using natural and synthetic coagulants aids, *J. Hazard Mater. B* 138: 40-45
- Adebowale K.O, E.I. Unuabonah, B.I Olu-Owollabi, (2008). Kinetic and thermodynamic aspects of the adsorption of Pb^{2+} and Cd^{2+} ions on tripolyphosphate-modified kaolinite clay. *Chemical Engineering Journal* 136 (2-3): 99-107
- Ademiuyi F.F, R.H. Gumus, S.M. Adeniyi, O.I. Jasem, (2009). Effect of process conditions on the characterization of activated carbon from waste Nigeria Bamboo, *Journal of Nigeria Society of Chemical Engineers*, 101, No 1& 2, pp 83-93.
- Aharoni C., M. Ungarish. (1977). Kinetics of activated chemisorptions part 2. Theoretical models, *J. Chem. Soc. Far. Trans. 73* (1977)pp. 456-464.
- Ajjiabi L.C. , L. Chouba.(2009). Biosorption of Cu^{2+} and Zn^{2+} from aqueous solutions by dried marine green macroalga chaetomorpha linum. *J. Environ. Manage*, 90: 3485-3489
- AL-Degs Y.S, M.A. Khraisheh, S.Y. Allen, M. Ahmad. (2000). Effect of carbon surface chemistry on the removal of reactive dyes from textile effluent, *Water Res.* 34(34), 927-935.
- Allen S. J., Q. Gan, R. Matthews, P.A. Jolinson.(2003). Comparison of optimized isotherm models for basic dye adsorption by kudu. *Bioresources Technology*, 8: 143-152.
- Allothman Z.A., M. Naushad, R. Ali, (2003). Kinetic, equilibrium isotherm and thermodynamic studies of Cr (VI) adsorption onto low-cost adsorbent developed from peanut shell activated with phosphoric acid. *Environ. Sci. Pollut. Res.* 20: 3351-3365.
- Aman T., A.A. Kazi, M.U. Sabri, Q. Bano, (2008). Potato peels as solid waste for the removal of heavy metal copper (II) from waste water/industrial effluent, *Colloids Surf. B: Biointerfaces* 63:116-121.
- Amosa M.K, M.F.R. Alkhatib, M.S. Jami, D.N. Jimat, R.U. Owolabi, S.A. Muyibi, (2014a). Morphological synthesis and environmental application of ZSM-5zeolite crystals from combined low-water and fluoride synthesis routes. *Advances in Environmental Biology*, 8:613-625

- Anirudhem T.S, P.G. Radhakrishnen, (2008). Thermodynamic and kinetics of adsorption of Cu (II) from aqueous solutions onto a new cation exchanger derived from tamarind fruit shell, J. Chen. Thermodynamic 40 (4): 702-709.
- APHA/AWWA (1995). Standard method for the Examination of Water and Wastewater. 9th ed. American Public Health Association, American water works Association and water Environment Federation . Washington DC., USA
- Arami M., N.Y. Limaee, N.M. Mahmoodi and N.S. Tabrizi. (2005). Removal of dye from colored textile wastewater by using orange peel adsorbent. Equilibrium and kinetic studies. Journal of collide and interface science, 288:371-376
- ASTM standard (1999). Standard test methods for moisture in activated carbon. Philiadephia, PA: ASTM committee on standard.
- ASTM D-3172-89, Standard Practice for proximate analysis
- Attia A.A, W.E. Rashwan, and S.A. Khedr, (2006). Capacity of activated carbon in the removal of acid dyes subsequent to its thermal treatment. Dyes and Pigments, 69 :128-136.
- Auta M., B.H. Hameed, (2011). Preparation of waste tea activated carbon using potassium acetate as an activating agent for adsorption of Acid Blue 25 dye, Chemical Engineering Journal. 171: 502-509
- Babel S., T.A. Kurniawan, (2003). Low-cost adsorbents for heavy metals uptake from contaminated water: a review. J. Hazard Mater. B97: 219-243
- Banker A.V., A.R. Kumar, S.S Ringarde, (2009). Removal of Cr (IV) ions from aqueous solution by adsorption onto two marine isolated of yawowialipolytical. J. Hazardous Materials, 170 pp. 487-494
- Bansal M., D. Singh, V.K. Garg and P. Rose, (2009). Use of agricultural waste for the removal nickel ions from aqueous solutions: Equilibrium and kinetics studies. International journal of Civil and Environmental and Engineering, 1(2):108-114
- Bhattacharya, G. Krishna, ArumimaShama, (2005). Kinetics and thermodynamic of methylene blue adsorption on neem (Azadirachtaindia) leaf powder. Dyes Pigment, 65. 1:51-59.
- Bhatnagar A., M. Sillanpaa., (2010). Utilization of agro-industrial and municipal waste materials potential adsorbent for water treatment. A review. Chem. Eng. J. 157: 277-296. <http://dx.Doi.org/10.1016/j.cej.2010.01.007>
- Budinova T., E. Ekinici, F. Yardim, A. Grimm, E. Bjornbom, V. Minkova, M. Goranova., (2006). Characterization and application of activated carbon produced by H₃PO₄ and water vapour activation. Fuel Process Technology, 87 :899-905.
- Chen H., and Y. Zhao, (2009). Adsorption study for removal of Congo Red Anionic Dyes using Organo-Attapulgite. Adsorption 15: 381-389.
- Cobas M., M.A. Sanroman, M. Pazos, (2014). Box-Bekin methodology for Cr(IV) and leather dyes removal by an eco-friendly biosorbent. F.versiculosus. Bioresour. Technol. 160:166-174
- Daifullah A.A.M., S. M. Yakout, S.A. Elreefy, (2007). Adsorption of fluoride in aqueous solution using KMnO₄ modified activated carbon derived from stem pyrolysis of rice straw. J. Hazard Mater. 147: 633-643
- Del Rio A.I., J. Fernandez, J. Molina, J. Bonastre, F. Cases , (2011). Electrochemical treatment of a synthetic wastewater containing a sulphonatedazo dye. Determination of naphthalenesulphonic compounds produced

- as main by-product. *Desalination* 273: 428-435
- Dio Y., W.P. Walawender, L.P. Fan, (2002). Activated carbon prepared from phosphoric acid activated of grain sorghum. *Biores. Technol.* 81:45-52
- Dogan M., Y. Ozdemin, M. Alkan, (2007). Adsorption kinetic and mechanism of cationic methyl violet and methylene blue dyes onto sepiolite. *Dyes Pigm* 75 :701-713
- Dubinin M.M., L.V. Radushkevich, (1947). The equation of the characteristic curve of the activated charcoal *Proc. Acad. Sci. USSR Phys.Chem. Soc.* 55 :331-337.
- EL- Guendi M.. Homogeneous surface diffusion model of basic dyestuffs onto natural clay in batch adsorbents. *Adsorption Science and Technology*, 8. (1991), 217-225.
- EL-hadad .E., (2012). Adsorption and Desorption processes of organic contaminants on carbonaceous material (Ph.D), Fac. Of Sci. Technische University pp.80
- EL-Sayed S.M.M, (2011). Physicochemical studies on the impact of pollution up on the River Nile Branches, Egypt (M.Sc thesis).Faculty of Science, Benha University, Egypt.
- Fomkin A, (2009). Nanoporous materials and their adsorption properties. *Institute of physical chemistry and Electrochemistry. Russian Academy of Science*, vol. 45, issue 2:133-149.
- Freundlich H.M.F., (1906). Over the adsorption in solution. *J. Phys. Chem.* 57 :385-471
- Garg V.K., M. Bansal, U. Garg and D. Singh, (2009). Removal of Cr (VI) from aqueous solutions using pre-consumer processing agricultural waste, A case study of rice Husk. *Journal Hazard Materials*, 162 (2009), 3125-3200.
- Gircis B.S., A.N.A. EL-Hendawy, (2002). Porosity development in activated carbons obtained from date pits under chemical activation with phosphoric acid. *Microporous and Mesoporous Materials*, 52,105-117.
- Gode .F, E. Petilivan. Removal of Cr (VI) from aqueous solution by two Lewitit anion exchange resin.
- Goldberg S., Equation and models describing adsorption processes in soil. *Soil science society of America*, 677S. Segoe Road, Madison, WI 53711, USA. *Chemical Processes in Soils. SSA Book series no. 8*
- Gomez G., M.S., M.P. Callao, (2007). Kinetic and adsorption study of acid dye removal using activated carbon. *Chemosphere* 69 (7) 1151-1158
- Gupta V.K, A. Rastogi. , (2009). Biosorption of hexavalent chromium by raw and acid-treated green alga *Oedogoniumhatei* from aqueous solutions. *J. Hazard Mater.*, 163: 396-402
- Haimour N.M., N. Emeish. (2006). Utilization of date stone for production of activated carbon using phosphoric acid. *Waste Management* 26 (6): 651-660.
- Hanafiah M.A.K, S. Shafiei, M.K. Harun, M.Z.A. Yahya. (2006a). Kinetic and thermodynamic study of Cd (II) adsorption onto rubber tree (*Hevea Brasiliensis*) leaf powder. *Journal of Applied science* 517 : 217-221.
- Hashem A., E. Abdel-Halim, H.A. Maaouf, M.A. Ramadan, A. Abo-Okeit., (2007). Treatment of saw dust with polyamine for wastewater treatment. *Energy Education Science and Technology*, vol.19 pp. 45-58.
- Hedazi H.A. Removal of heavy metal from wastewater using agriculture and industrial wastes as adsorbent. *HBRC J.9*, 276-282
- Hema M., S.Arivoli., (2007). *International Journal of Physical Science* vol. 2(1), pp. 010-017.
- Hobson J.P.,(1969). Physical adsorption isotherms extending from ultra -high vacuum to vapour pressure, *J. Phys. Chem.* 73:2720-2727.

- Hossain M.A., H.H. Ngo, W.S. Guo, T.V. Nguyen. (2012). Palm oil fruit shells as biosorbent for copper experiments and sorption models. *Bioresour. Technol.* 113: 97-101.
- Hussans G., M.A. Khan., (2011). Adsorption of gold (III) from aqueous solution on bagasses Ash. *Journal of chemical society of Pakistan*, 33: 317-323.
- Hutson N.D., R.T. Yang., (2000). Adsorption, *J. Colloid Interf. Sci.*, pp. 189.
- Imamoglu M., O. Tekir. (2008). Removal of copper (II) and Lead (II) from aqueous solutions by adsorption on activated carbon from a new precursor hazelnut husks. *Desalination*, 228 (1-3): 108-113
- Ismail B., S.T. Hussain and S. Akram. , (2013). Adsorption of methylene blue onto spinel magnesium aluminate nanoparticles, Adsorption isotherms, kinetic and thermodynamic studies. *Chemical Engineering Journal* 219 (2013), 395-402
- Jaman H., D. Chakraborty, P. Saha. (2009). A study of the thermodynamic and kinetics of copper adsorption using chemically modified rice husk. *Clean* 37: 704-711.
- Jambulingam M., S. Karthikeyan, P. Sivakumar, J.Kiruthithika and T. May alagan. (2007). Characteristic study of some activated carbons from agricultural wastes, *Journal of scientific and industries research*, 66 :495-500
- Jayaram K., I.Y.L.N. Murthy, H. Lallunaituanga, M.N.V. Prasad., (2009). Biosorption of lead from aqueous solution by seed powder of *strychrospotonium L.* *Colloid Surf.B.*, 71 (2): 248-254.
- Ketcha J.M., D.J.D. Dina, H.M. Ngomo, N.J.Ndi. (2012). *Am. Chem. Sci. J.* 2:136-160.
- Khan T.A., V.V. Singh, S. Sharma. (2009) Elimination of heavy metals from wastewater using agricultural wastes as adsorbents. *Malaysian Journal of science.* 23: 43-51
- Khataee A.R., G. Dehghan. (2011). Optimization of biological treatment of a dye solution by macroalgecladophora sp. using surface methodology. *J Taiwan Inst. Chem. Eng.* 42 :26-33
- Krishani K.K., X. Meng, C. Christodoulatos, V.M. Boddu.(2006). Biosorption mechanism of nine different heavy metals onto biomatrix from rice husk. *J.Hazard. Mater.* 153: 1222-1234.
- Krishnan A.K., K.G. Sreejalekshmi and V. Sumol., (2010). Adsorptive retention of citric acid onto activated carbon prepared from HareaBrazillians sawdust, kinetic and isotherm overview. *Desalination* 257: 46-53.
- Kundu S., A.K. Gupta. (2006). Arsenic adsorption onto iron- oxide- coated cement (IOCC). Regression analysis of equilibrium data with several isotherm models and their optimization. *Chem Eng. J.*, 122: 93-98
- Langmuir I. (1916). The constitution and fundamental properties of solids and liquids , *J. Am. Chem. Soc.* 38:2221-2295
- Larous S., A.H. Meniai, M.B. Lehocine.,(2005). Experimental study of the removal of copper from aqueous solutions by adsorption using sawdust, *Desalination* 185: 483-490.
- Liang S., K. Guo, W. Feng, O. Tian. (2009). Application of orange peels xanthate for the adsorption of Pb (II) from aqueous solutions *J. Hazardous materials.* 176, pp. 425-429
- Lugo-Lugo V., S. Hernandez-Lopez, C. Barrera – Diaz., (2009). A comparative study of natural foraldehyde- treated and copolymer grafted orange peel for Pb (II) adsorption under batch and continuous mode. *J. Hazard Mater.* 161 (2-3) 1255- 1264.
- Ma W., P. Zong, Z. Cheng, B. Wang, Q. Sun. (2014). Adsorption and bio-sorption of nickel ions and reuse for 2-Chlorophenol catalytic ozonation oxidation degradation from water. *J. Hazard.Mater.* 266 :19-25.

- Mahmut Ozacar, I. AyhamSengil., (2003). Adsorption of reactive dyes on calcinedalvnite from aqueous solution. *Journal of Hazardous Materials*, 98. 1, (2003), 211-224.
- Mall I.D., C. Vimal, Srivastava, K. Nitim, Agarwal. (2006). Removal of Orange-G and methyl Violet dye by adsorption onto bagasse fly ash- kinetic study and equilibrium isotherm analysis, *Dyes and Pigment* 69.3, 210-223.
- Mohammad AL-Amber.(2010). Removal of high-level Fe^{3+} from aqueous solution using Jordanian inorganic materials: Bentonite and Quartz, *Desalination* 250: 885-891.
- NageswaraRao M., C.H. Chakrapani, B.V. Rajeswara Reddy, C.H. Suresh Babu, Y. HanumanthaRao, K. SomasekharaRao, K. Rajesh. (2011). Preparation of activated Kazas carbons from bio-materials and their characterization. *Int. J. Appl. Biol. Pharm. Tech.* 2 (3): 610-618.
- Namasivayam C., Dyes Kavith. (2002). Removal of Congo Red from water by adsorption onto activated carbon prepared from coir pith, an agricultural solid waste. *Dyes and Pigment* 54,(1) :47-58
- Nandi B.K., A.W. Goswami and Purkait. (2009). Adsorption characteristic of brilliant green dye on kaolin. *Journal of Hazardous Materials*. 161, 1: 387-395.
- Nethaji S., A.Sivasamy, G. Thennarasu, S. Saravanam. (2010). Adsorption of Malchite green dye, onto activated carbon derived from *Borassusaethiopum* flower biomass, *J.Hazard Mater.* 181: 271-280.
- Nguyen T.A.H., H.H. Ngo, W.S.Guo, L. Zhang, Q.Y. Yue, Q. Li, T.V. Nguyen. (2005). Applicability of agricultural waste and by-products for adsorptive removal of heavy metals from wastewater. *Bioresour. Technol.* 148,(2013), 574-585 *J. Hazard Mat.* B119, pp. 175-182
- Oguz E. (2005). Adsorption characteristics and kinetics of the Cr (VI) on the *ThujaOrientalis*. *Colloids and surfaces A: Physicochemical and Engineering Aspects*, 252: 121-128.
- Ozcimen D., A. Ersoy-MeridoYu. (2010). Adsorption of copper (II) ions onto Hazelnut shell and Apricot stone activated carbons. *Adsorption Science and Technology*, 28: 327-340. <http://dx.doi.org/10.1260/063-617.28.4.327>
- PadillaE. Padilla-Ortega, R. Leyva-Ramos, J.V. Flores-Cano. (2013). Binary adsorption of heavy metals from aqueous solution onto natural clays. *Chem. Eng. J.* 225: 536-546.
- Park D., S.R. Lim, Y-S. Yun, J.M. Park. (2008). Development of a new Cr(VI) biosorbent from agricultural biowaste. *Bioresour. Technol.* 99: 8810-8818.
- Phan N.H., S. Rio, C. Faur, L. Le Coq, P. Le Cloirec, T.H. Nguyen. (2006). Production of fibrous activated carbons from natural cellulose (jute coconut) fibers for water treatment-applications, *Carbon* 44: 269-277.
- Prahas D., Y. Kartika, N. Indraswati, S. Ismadji.(2008). Activated carbon from jackfruit peel waste by H_3PO_4 chemical activation: Pore structure and surface chemistry characterization. *Chemical Engineering Journal* 140 :32-42.
- Preethi S, Sivasamy, (2006). *Ind. Eng. Chem. Res.* 45 : 7627-7632
- Remero-Gonzalez Y., Y.R. Peralta-vidua, E. Rodriguez, S.L.J.L. Ramirez. (2005). Determination of thermodynamic parameters of Cr(VI) adsorption from aqueous solution onto *Agave lechuguilla* biomass. *Journal of Chemical Thermodynamic*, 37 :343-347.
- Rosales E., M. Pazos, M.A. Sanroman, T. Tavares. (2012). Application of zeolite-Arthrobacter viscous system for the removal of heavy metal and dye. *Chromium and azure B. Desalination* 284:150-156
- Safa Y., H.N. Bhatti. (2011a). Adsorptive removal of Direct Dyes by low-cost rice husk, *Effect of*

- treatments and modification. African Journal of Biotechnology, 10 (6):28-3142.
- Senthilkumar S., P. Kalaamani, P. Porkodi, P.R. Varadarajan, C.V. Subburan. (2006). Adsorption of dissolved red dye from aqueous phase onto activated carbon prepared from agricultural waste, BioresourcesTechnol, 97(4), 1618-1625.
- Shama S.A., M.A. Gad. (2010). Removal of heavy metals (Fe^{3+} , Cu^{2+} , Zn^{2+} , Pb^{2+} , Cr^{3+} and Cd^{2+}) from aqueous solutions by using hebbra clay and activated carbon. Port. Electrochim.Acta 28 (4), 231-239
- Sharma I., D. Goyal. (2009). Kinetic modeling: Chromium (III) removal from aqueous solution by microbial waste biomass. J. Sci. Ind. Res., 68 :640-646
- Singanan M., (2011). Removal of Lead (II) and Cadmium (II) ions from wastewater using activated biocarbon. Sci. Asia 37 : 115-119.
- Srivasta V.C., I.D. Mall, I.M. Mishra.(2006). Characterization of mesoporous rice husk ash (RAH) and adsorption kinetic of metal ions from aqueous solution onto RHA. J. Hazard. Mater. B134, 257-267.
- Tan I.A.W., A.L. Ahmad, and B.H. Hameed. (2008). Adsorption of basic dye on high-surface-area activated carbon prepared from coconut husk: equilibrium, kinetic and thermodynamic studies, Journal of Hazardous Materials 154(1-3):337-346.
- Taty-Costode V.C. Taty-Costodes, H. Fauduet, C. Porte, A. Delacroix. (2003). Removal of Cd (II) and Pb (II) ions, from aqueous solutions, by adsorption onto sawdust of *Pinus sylvestris*. J. Hazard Mater. 105:121-142
- Temkin M.I., V. Pyzhev. (1940). Kinetic of ammonia synthesis on promoted iron catalyst. ActaPhysiochem. USSR, 12: 217-222.
- Tongpoothorn W, M. Sriuttha, P. Homchan, S. Chanthai, C. Ruangviriyachac. (2011). Preparation of activated carbon derived from jatrophacurcas fruit shell by simple thermochemical activation and characterization of their physic-chemical properties, Chemical Engineering Research and Design, 89 (3): 335-340.
- ValentaNabais J.M., J.A.G. Suhas, P.J.M. Carrott, C. Laginhas, S. Roman. (2009). Phenol removal onto novel activated carbons made from lignocellulosic precursors: influence of surface properties; J. Hazard Mater. Vol. 167, pp. 904-910.
- Weng C.H., C.P. Huang. (2004). Adsorption characteristics of Zn (II) from dilute aqueous solution by fly ash. Colloid. Surf. A, 247 (1-3) :137-143.
- Xiong C., C. Yao, L. Wang, J. Ke. (2009). Adsorption behavior of Cd from aqueous solution onto gel-type weak acid resin. Hydrometallurgy 98: 318-324
- Yasemin B., T. Zeki. (2007). Adsorption study on ground shells of hazelnut and almond, Journal of Hazardous Materials, vol. 149,pp. 35-41.
- Yun C.H., Y.H. Park, C.P. Park, (2008). Effects of pre-carbonization on porosity development of activated carbons from rice straw. Carbon, 39: 559-567.
- Zhang B., R. Fan, S. Wang, L. Wang, J. Shi., (2013). Biosorption characteristic of *Bacillus gibsonii*-2 waste biomass for removal of lead (II) from aqueous solution. Environmental Science and international Pollution Research. 20: 1367-1373